Essential Readings in Light Metals: Electrode Technology for Aluminum Production.
Edited by Alan Tomsett and John Johnson.

From ***Light Metals 1984***, J.P. McGeer, Editor

CHEMICAL RESISTANCE OF CATHODE CARBON MATERIALS DURING ELECTROLYSIS

Morten Sørlie* and Harald A. Øye

Institutt for uorganisk kjemi
Norges tekniske høgskole
Universitetet i Trondheim
N-7034 Trondheim-NTH, Norway.

Commercial cathode materials for use in Hall-Heroult electrolysis are characterized physicochemically and the properties are correlated with deterioration resistance *versus* sodium vapour and interaction with melt-liquid aluminium. Resistant materials were characterized by the (002) X-ray peak, the crushing strength and the porosity. An unsuccessful attempt to graphitize anthracite by interaction with sodium vapour is described. Finally, penetration velocities and profiles are given and discussed.

Introduction

This work is part of a study of the deterioration mechanism of cathode carbon during aluminium electrolysis. A literature survey has been given in Metall [1] while the first account on our experimental work was presented at the 1982 AIME Annual Meeting [2]. A more extensive account of the relationship between physicochemical properties and resistance towards sodium attack is recently printed in Metall [3].

Failures associated with the cathode carbon lining are the most common causes for discontinued production in aluminium reduction cells. During electrolysis sodium and electrolyte are continuously being absorbed by the carbon lining, creating problems of swelling, cracking, arching, heaving and crumbling of the cathode.

The aim of the present study is to find correlations between physicochemical properties of the cathode carbon and its resistance towards deterioration by sodium attack and penetration by sodium and bath. Some experiments to study a possible sodium induced graphitization are also described.

Characterization of laboratory cathodes and their resistance towards sodium

The cathodes employed were either fabricated in the laboratory from green cold type tamping mix [2,4] or made from cores drilled out of prebaked cathode blocks. The finished cathode had a diameter of 25 mm and a length of 60-75 mm. In order to cover a broad range of industrially important carbon qualities we have included four different cold type tamping pastes and four different prebaked cathode blocks. Physicochemical properties are given in Table 1. The numbering of the materials is the same as in ref. [3]. All are commercially available and currently used in the aluminium smelting industry. The resistance of the various materials towards cracking and exfoliation due to sodium attack are also listed in Table 1.

Two of the materials (*M-V*, *B-VIII*) may be regarded as highly graphitic and can be classified as being strongly resistant to chemical deterioration from sodium attack. A partly graphitized anthracite (*M-I* and *B-III*) has a far better sodium resistivity than a partly graphitized calcined coke (*M-IV*) [3] which is very susceptible to sodium cracking and exfoliation. The amorphous anthracitic material *M-II* also shows a poor resistance towards sodium. The block materials *B-II* and *B-IV* have intermediate properties.

There is no single material parameter which can determine the suitability of material in the aluminium smelter cathode [3]. With a few exceptions, strength appears to be inversely related to the graphite content and it is of interest to observe that the material which showed the poorest sodium deterioration resistance (*M-II*) originally had a particularly high crushing strength (Table 1). The inferior materials *M-II*, *B-II* and *B-IV* did also have a low porosity.

Usual X-ray characteristica could not readily be employed for characterization of the chemical resistivity of anthracitic cathode carbon materials [3]. Neither graphitization index nor mean stacking height of layer planes (L_c) appeared to be applicable for evaluation of deterioration resistivity with respect to cathode carbons. Neither did the asymmetry of the most important diffraction peak give any clear indication of the graphite content. However, a X-ray diffraction intensity ratio between a natural graphite standard and the tested material gave a correlation between the anthracitic cathode carbon materials and the observed deterioration resistances [3]. The inferior materials, seam mix *M-II* and carbon blocks *B-II* and

B-IV, have (002) intensity ratios less than or equal to 0.02 while acceptable materials have ratios larger than or equal to 0.06. The seam mix of calcined coke origin (*M-IV*) again does not fit into the pattern and will probably remain susceptible to chemical deterioration unless it is more fully graphitized.

In Situ graphitization of aluminium smelter cathodes

It has been known that aluminium smelter linings graphitizes with age [5,6] and that after a period of about 1 year, the anthracite filler is nearly completely converted to graphite [7]. Dell [5] found that the graphitization of the lining was equivalent to that of anthracite heated to 2500°C.

The operating temperature of a Hall cell is about 970°C and there is no evidence which supports that the lining or part of it ever comes anywhere near thermal graphitizing temperatures. The ordering process which takes place at temperatures 850-1000°C must be catalyzed and the intercalation of sodium into the carbon structure is believed to play a crucial part as it modifies the carbon structure and enlarges the distance between the graphite layers adjacent to the intercalation sites [1].

Short time exposure of anthracite to sodium vapour was not found to lead to graphitization [8], but Rapoport [9] reported structural ordering in anthracite to take place during laboratory electrolysis experiments where samples were cathodically polarized for up to 95 h with temperature fluctuations of 100°C. The reason for this was believed to be the repeated formation and decomposition of sodium intercalation compounds caused by the temperature cycling.

The exposure of anthracite to sodium vapour at 833°C (the b.p. of sodium) was shown to cause extensive damage due to swelling and exfoliation [2]. Experiments were therefore initiated to test if long term exposure to sodium had any influence on the structural ordering of anthracite. Samples of calcined amorphous anthracite were together with sodium metal sealed under argon atmosphere in heavy wall cylindrical steel vessels (by welding). The steel cylinder was placed in an alumina crucible and the assembly was finally sealed in quartz ampoules under vacuum. The samples were kept in a furnace where the temperature was allowed to cycle 15°C around 883°C, the boiling point of sodium metal. Samples were removed at regular intervals, cut open and the carbon content analyzed by X-ray diffraction after removal of its sodium content by acid leaching. Over a period of 10 months no structural changes detectable by X-ray diffraction analysis were found.

These results seem to exclude that the low temperature graphitization of aluminium smelter linings is caused solely by the mechanism of cyclic formation and decomposition of sodium intercalation compounds. These results lend support to the mechanism suggested by Waddington [6]. He observed that graphitization only seemed to occur in the parts of the cathode which had been penetrated by both sodium metal and molten electrolyte and not in sections where only sodium metal was present. Based on this he proposed that the carbon first was converted into a lamellar compound by the penetrating sodium vapour and then later, when liquid bath reached the compound, it decomposed with the formation of graphitic material [6]. The carbide forming reaction may well be the decomposition step.

$$4Na_3AlF_6 + 12Na + 3C = Al_4C_3 + 24NaF \qquad (1)$$

Table 1. Physico-chemical properties and sodium resistance of cathode carbons.

	Cold type tamping paste				Prebaked cathode blocks			
Carbon filler material	*M-I*	*M-II*	*M-IV*	*M-V*	*B-II*	*B-III*	*B-IV*[a]	*B-VIII*
	Anthracite, partly graphitized	Anthracite, calcined but highly amorphous with respect to X-ray diffraction	Soft and partly graphitized calcined coke filler	Highly graphitic	Anthracite, partly graphitized			Highly graphitic
PHYSICOCHEMICAL PROPERTIES								
Ash content (%)	1.9	4.4	0.41	0.32	5.2	3.7	3.6	0.03
Porosity (%)	18.6	14.4	25.7	33.4	9.9	18.6	11.1	21.1
Crusning strength (N/mm^2)	15	60	37.5	8.5	28	21	52	25
d_{002} (Å)	3.3684	b)	3.3797	3.3684	3.3797	3.3797	3.3671	3.3671
Graphitization index	0.83	b)	0.70	0.83	0.70	0.70	0.85	0.85
L_c (Å)	177	b)	107	62	83	100	180	63
(002) intensity ratio	0.08	0	0.17	0.46	0.02	0.06	0.02	0.40
RESISTANCE TOWARDS SODIUM ATTACK								
CR ratio								
Crucible ∞ (NaF)	*	***	***	-	**	**	**	-
test, 4.0	*	**	**	-	*	-	*	-
1000°C 3.2	-	**	*					
3.0 (Na_3AlF_6)	-	*	*		*		*	
2.5	-	*	*					
1.5	-	-	-					
Sodium vapour test, 883°C	*	***	***	-	**/***	*	**/***	-

a) Sidewall blocks; b) Can not be determined; ***: Extreme cracking and exfoliation; **: Heavy to moderate cracking; *: Hairline cracks, little damage; -: No effect.

Penetration of sodium and bath during reversed polarity electrolysis

Electrolysis were carried out at 1000°C and the parameters varied were electrolyte cryolite ratio (CR)*, current density (CD) and duration of electrolysis. The experiments were performed in the reversed polarity apparatus which has been described previously [2].

After removal of excess electrolyte or cathodic deposits [4] from the cathode surface, the cathodes were cut into 3-5 mm thin discs. One surface of these discs was then analyzed for sodium, aluminium and fluorine by means of X-ray fluorescence spectroscopy. It was important to perform these analyses as quickly as possible after cutting the cathode, as sodium metal which was present in the carbon lattice readily oxidized near the surface. Due to its hygroscopy and subsequent volume expansion it could else accumulate on the surface as sodium hydroxide.

The X-ray fluorescence analyses gave concentration profiles like those shown in Figures 1 and 2. Cryolite (Na_3AlF_6) was used as an analytical standard and the values given are net concentrations. Any sodium and aluminium which might have been present as mineral impurities (ash) were subtracted from the results by using a dummy sample made of the same unelectrolyzed carbon material. Due to its low atomic number the fluorine X-ray analysis is believed to give the least accurate values.

The concentration profiles shown in Figures 1 and 2 correspond qualitatively to those earlier presented by Dell [5] which show that sodium usually was the diffusing atom with the highest concentration in carbon. The sodium concentration profile consists of two superimposed sodium waves, firstly the metallic sodium which migrates through the carbon lattice by means of an intercalation mechanism [2], then secondly follows the diffusion of molten bath by capillary attraction through the open porous network of the carbon specimen. The migration of this second wave is probably made possible by changes in bath/carbon wetting conditions caused by changes in surface properties of the sodium-carbon compound. The form of the concentration profiles was explained by Dewing [10] to be caused by the deposition of aluminium carbide on the pore walls by reaction between migrating cryolite, carbon and intercalated sodium metal (Equation (1)). The solid aluminium carbide does not migrate further into the carbon but is deposited near the surface, while the liquid electrolyte with increased excess of sodium fluoride continues to migrate through the electrode in the wake of the sodium metal front. Figure 3 shows photographs from an electron microprobe analysis of a cylindrical carbon electrode (cathode) cut perpendicular to its axis. The metallic sodium wave has already passed through this plane and the molten electrolyte, now completely depleted of aluminium fluoride, has just started to penetrate. A vein of nearly pure sodium fluoride formed according to Equation (1) can be seen at the upper right hand side corner (BSE, Na, and F images).

The electrode in Figure 3 is the *M-I* type made with a partly graphitized anthracitic filler. From the sodium X-ray emissions (which density is approximately proportional to the sodium concentration) it can be seen that the sodium concentration is larger near the grain boundaries of the filler grains than within the particles. This is contrary to what was found in cases where the carbon aggregate was made of a low calcined amorphous anthracite [2]. In that case it was shown that sodium had an equally high prefe-

*CR = mol NaF/mol AlF_3. Acidic compositions at CR < 3.0; basic at CR > 3.0.

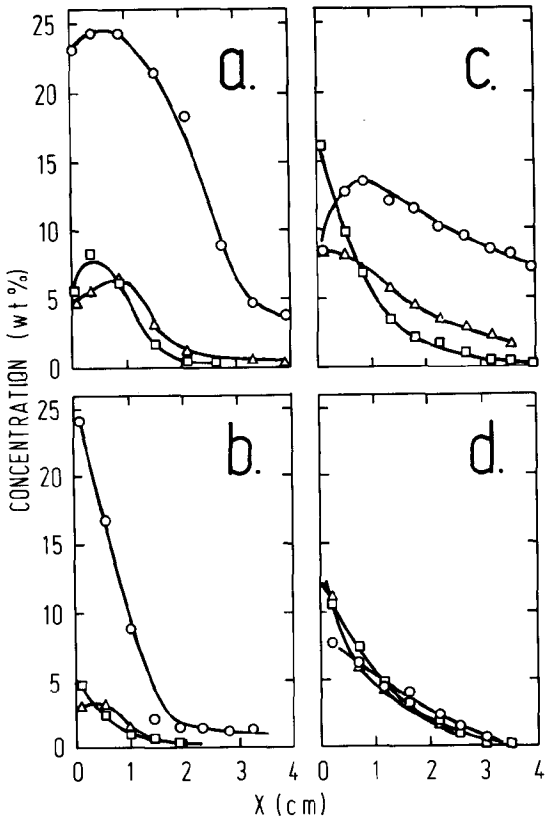

Figure 1. Concentration profiles after 4 h electrolysis at 1000°C using seam mixes *M-II* and *M-V* as cathode materials.
o: Na; □: Al; Δ: F.

a. *M-II*
CD = 0.43 A/cm^2
CR = 4.0

b. *M-II*
CD = 0.43 A/cm^2
CR = 1.5

c. *M-V*
CD = 0.46 A/cm^2
CR = 4.0

d. *M-V*
CD = 0.46 A/cm^2
CR = 1.5

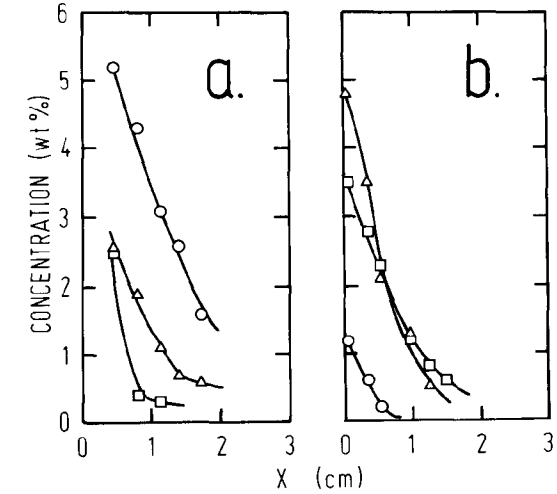

Figure 2. Concentration profiles in *B-VIII* prebaked cathode block after electrolysis at 1000°C with CD = 0.15 A/cm^2.
o: Na; □: Al; Δ: F.

a. CR = 4.0, 4 h

b. CR = 1.5, 2 h

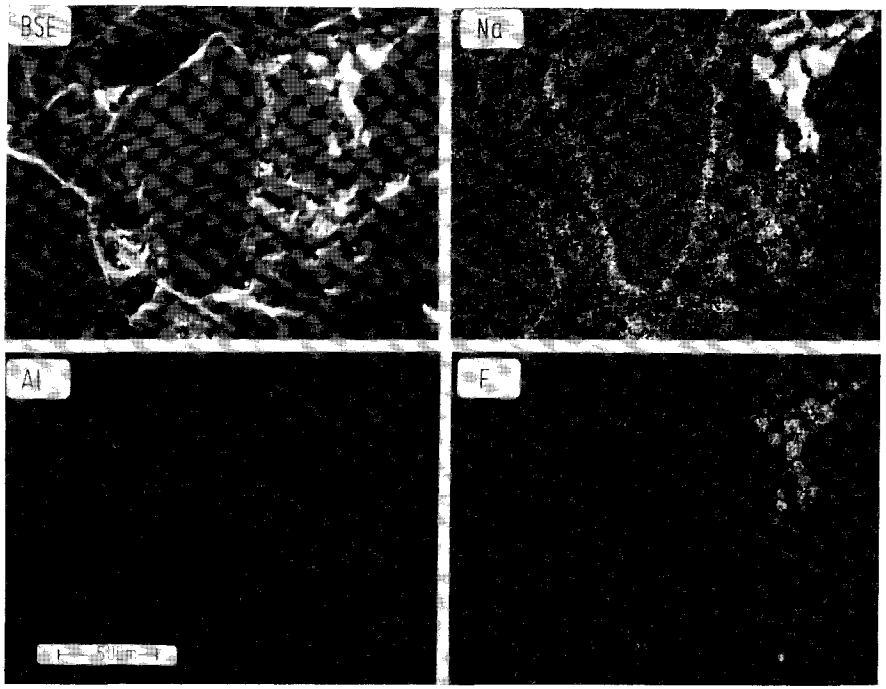

Figure 3. Qualitative microprobe analysis of *M-I* carbon electrode after electrolysis. The photographs shown are backscatter electron (BSE) together with sodium, aluminium, and fluorine X-ray emission images.

rence for the non-porous anthracite grains as for the highly porous binder coke. In the partly graphitized *M-I* filler (Figure 3) the better ordering of the lattice has made the anthracite less susceptible to sodium penetration than the binder coke.

The concentration profiles in Figures 1 and 2 tell about the ease with which sodium metal and electrolyte penetrate into various cathode carbon materials. Sodium penetrates anthracite easily (Figures 1a,b) and the melt follows slowly in the wake of a high concentration of sodium metal. Graphite is much more resistant towards sodium metal intercalation (Figures 1c,d) and the sodium metal wave is not as pronounced here and the bath components follow more closely, but due to its higher open porosity (Table 1) more melt can accumulate. In Figure 1d (graphite *M-V*, acidic melt) it is not possible to distinguish the sodium metal front from that of the migrating bath. This is further emphasized in Figure 2 (prebaked graphitic cathode block *B-VIII*) where the melt penetration closely follows the sodium metal front. In the acidic melt the concentration of fluorine has even become higher than the total sodium concentration and reflects roughly the melt composition near the electrolyte surface.

Sodium metal and electrolyte diffusion in cathode carbons

Previous work [2] indicated that diffusion was the mechanism by which sodium metal and melt migrated through the lattice. By considering the cathode as an infinite solid and assuming a constant activity of sodium metal at the electrolyte/carbon interface during electrolysis (or an infinite reservoir of diffusing species), the square of the diffusion length along the axis of the electrode, measured at a constant concentration of the diffusing species, is a linear function of the diffusion time, t [11]. The solution to Fick's law

$$\frac{\partial c}{\partial t} = D \frac{\partial^2 c}{\partial x^2} \qquad (2)$$

under the above circumstances is

$$\frac{c_i - c_x}{c_i - c_0} = \frac{2}{\pi^{\frac{1}{2}}} \int_0^k e^{-y^2} dy \qquad (3)$$

where

$$k = \frac{x}{2(Dt)^{\frac{1}{2}}} \qquad (4)$$

c_i = concentration of diffusing species at the interface x = 0 which during electrolysis is assumed to be constant; c_x = concentration at diffusion depth x at time t; c_0 = concentration (constant for all x) at the beginning of diffusion. By measuring x as a function of t at constant c (c_x = cut-off concentration) the left hand side of Equation (3) is constant. This means that also the right hand side of Equation (2) and thus k is constant. A plot of x^2 *versus* t should then yield a straight line for all diffusion controlled processes.

The quick method by cutting the laboratory cathode along its axis and measuring the penetration depth of sodium metal by pressing the exposed surface towards a paper wetted by phenolphthalein acid/base indicator [2] proved to be a quite accurate way of determining the diffusion depth of Na metal in anthracitic materials (at a constant cut-off concentration). Remeasurements by means of X-ray fluorescence techniques of the same cathode materials subjected to the same experimental conditions gave nearly identical curves at a cut-off concentration of 3 wt% Na. All further discussion is referred to this cut-off concentration.

Figures 4-6 show the penetration of sodium in the amorphous low calcined anthracite (*M-II*) as a function of current density and cryolite ratio. Figure 4 shows that the penetration follows Equation (3) and that the penetration velocity is highest at the highest current density.

During electrolysis sodium is formed at the electrode either by a primary charge transfer reaction or from the equilibrium

$$3NaF + Al = AlF_3 + 3Na \qquad (5)$$

Equation (5) is shifted towards the right hand side in basic melts, thus increasing the interfacial concentration of sodium, c_i, in Equation (2). More sodium penetrates the electrode in a given time thus moving the constant cut-off concentration further into the carbon material. This is illustrated in Figure 5 where the sodium penetration depth into amorphous anthracite (*M-II*) increases markedly as the cryolite ratio increases. The change is most pronounced in the acidic region. The movement of the sodium front

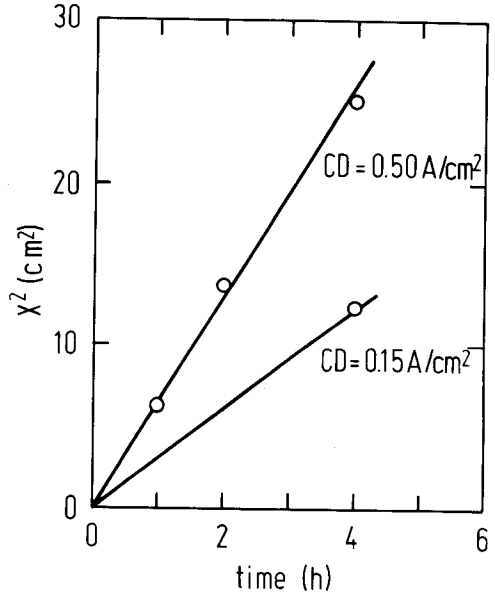

Figure 4. Square of sodium metal penetration depth (3 wt% cut-off) plotted *vs.* electrolysis time at 1000°C with CR = 4.0 using amorphous anthracitic seam mix *M-II* as cathode.

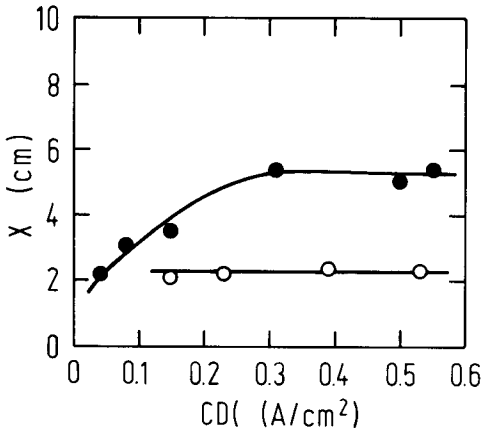

Figure 6. Sodium penetration (3 wt% cut-off) in *M-II* during 4 h electrolysis at 1000°C at various CD's.

●: CR = 4.0
o: CR = 1.5

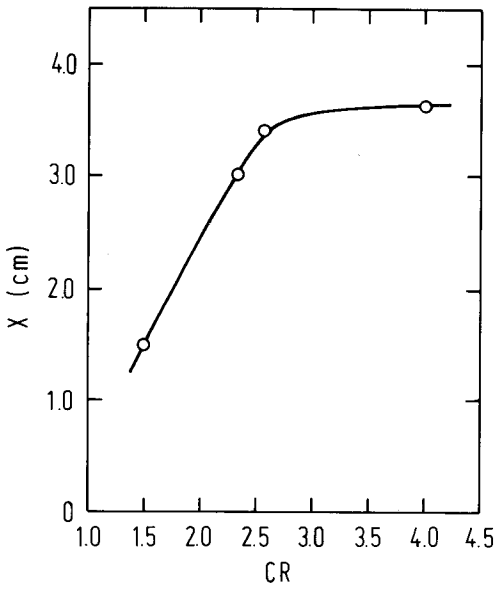

Figure 5. Penetration depth of sodium in *M-II* electrode (3 wt% cut-off) during electrolysis for 4 h at 1000°C, CD = 0.15 A/cm^2 in cryolite electrolytes of varying acidity.

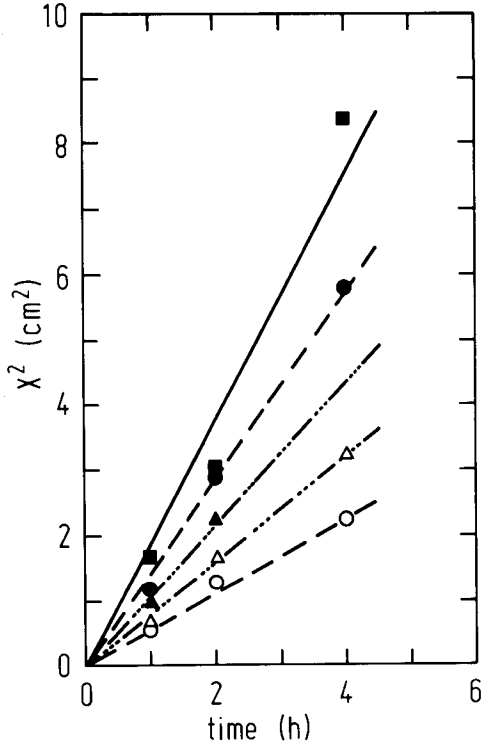

Figure 7. Square of sodium penetration depth (3 wt% cut-off) in three graphitic or partly graphitic seam mix cathodes plotted *vs.* electrolysis time at 1000°C with CD = 0.15 A/cm^2.
Open symbols: CR = 1.5.
Filled symbols: CR = 4.0.

o,● -------: *M-I*
■ ————: *M-IV*
Δ,▲ —·—·—: *M-V*

further into the carbon is caused by the increased sodium equilibrium concentration at the interface. At basic compositions the curve seems to flatten out. Due to a high sodium activity in the basic melt, combined with a rapid removal of sodium by intercalation into the carbon, the presence of liquid aluminium can no longer be maintained at the electrode surface at low CD's.

This is also apparent when the current density is varied (Figure 6). It is evident that a constant sodium activity (*i.e.* presence of aluminium metal) at the electrode/bath interface is reached at CD = 0.3 A/cm^2 in the basic electrolyte CR = 4.0 while aluminium metal appears to be present below CD = 0.15 A/cm^2 in the acidic CR = 1.5.

Penetration time to a depth of 30 cm into various carbon materials is calculated in Table 2. The highest sodium penetration rate is

Table 2. Time calculated for sodium (3 wt% cut-off concentration) to penetrate a 30 cm high carbon slab at 1000°C.

CD (A/cm^2)	CR	*M-I*	*M-II*	*M-IV*	*M-V*	*B-III*	*B-VIII*
		Time (days)					
0.15	1.5	67	67		47		>200
	4.0	26	12	20	35	27	109
0.50	4.0		6				

found in amorphous low calcined anthracite (*M-II*) while the slowest migration is observed in the prebaked graphitic cathode block (*B-VIII*).

The penetration of sodium into some of the partly graphitized cathode blocks is shown in Figure 7. The penetration velocity follows Equation (3) but the penetration mechanism is more complex. These materials are more porous than the amorphous anthracite (Table 2) and the total movement of sodium (metallic or ionic) is due to an interplay of intercalation and movement of melt in pores.

In basic melts (high activity of metallic sodium) it is seen from Figure 7 that the penetration velocity is lowest in the highly graphitic material *M-V*. The penetration is higher for the partly graphitized material *M-I* and still higher for the material made from calcined coke (*M-IV*).

In acidic melts the penetration velocity of sodium is as expected lower for all materials but the order is reversed, *M-V* > *M-I*. This latter order is, however, the order of porosity and the reversed sequence is probably due to that the measured Na cut-off (3 wt%) is a cut-off for melt movement, the melt moving more easily in the more porous material. As already mentioned this is also indicated in Figure 1 where the melt is trailing behind metallic sodium in the amorphous material (Figures 1a,b) and for basic melts in the graphitic material (Figure 1c), while sodium, aluminium and fluoride are moving close together in graphitic carbon when the melt is acidic (Figure 1d).

Acknowledgement

We wish to thank Bente M. Faaness for experimental assistance and the *Royal Norwegian Council for Scientific and Industrial Research (NTNF)* and the *Norwegian aluminium industry* for financial support.

References

1. M. Sørlie and H.A. Øye, Metall 36 (1982) 635.
2. C. Krohn, M. Sørlie, and H.A. Øye, Light Met., Proc. Sess. AIME Annu. Meet., 111th (1982) 311.
3. M. Sørlie and H.A. Øye, Metall 37 (1983.
4. O. Herstad, C. Krohn, M. Sørlie, and H.A. Øye, Aluminium 59 (1983) 200.
5. M.B. Dell, in Extractive Metallurgy of Aluminium, Vol. 2, ed. by G. Gerard, Interscience Publishers, New York, 1963, p. 403.
6. J. Waddington, in Extractive Metallurgy of Aluminium, Vol. 2, ed. by G. Gerard, Interscience Publishers, New York, 1963, p. 435.
7. W.E. Haupin, Aluminium 52 (1976) 446.
8. J.G. Hooley and P.T. Hough, Ext. Abstr. Program - Bienn. Conf. Carbon, 13th (1977) 454; 14th (1979) 286.
9. M.B. Rapoport, I.M. Maltseva, and M.L. Bluyshtein, Dokl. Chem. Technol. (English translation) 177 (1967) 180.
10. E.W. Dewing, Trans. Met. Soc. AIME 227 (1963) 1328.
11. A. Tiselius, Z. Phys. Chem. 169A (1934) 425.